Металлофиз. новейшие технол. / Metallofiz. Noveishie Tekhnol.
2005, т. 27, № 5, сс. 625–634
Оттиски доступны непосредственно от издателя
Фотокопирование разрешено только
в соответствии с лицензией

© 2005 ИМФ (Институт металлофизики
им. Г. В. Курдюмова НАН Украины)

Напечатано в Украине.

МЕТАЛЛИЧЕСКИЕ ПОВЕРХНОСТИ И ПЛЁНКИ

PACS numbers: 66.30.Jt, 68.35.Fx, 68.37.Ps, 68.49.Sf, 68.55.Ln, 68.60.Dv, 82.80.Yc

Effect of Nitrogen in Ta–Si–N Thin Films on Properties and Diffusion Barrier Performances

A. V. Kuchuk, V. P. Kladko, V. F. Machulin, O. S. Lytvyn,
A. A. Korchovyi, A. Piotrowska[*], R. A. Minikayev[**], and R. Jakiela[**]

V. E. Lashkaryov Institute of Semiconductor Physics, N.A.S.U.,
Nauka Prospekt, 41,
03028 Kyyiv, Ukraine
[*]*Institute of Electron Technology,*
Al. Lotnikow, 32/46,
02-668 Warsaw, Poland
[**]*Institute of Physics, Polish Academy of Sciences,*
Al. Lotnikow, 32/46,
02-668 Warsaw, Poland

Thin films of binary Ta–Si and ternary Ta–Si–N are deposited by reactive r.f. magnetron sputtering of a Ta_5Si_3 target within the N_2/Ar ambient. The role of composition in the resistivity, microstructure, and thermal stability of sputtered Ta–Si–N films is studied using the Rutherford backscattering spectrometry, X-ray diffraction, secondary-ion mass spectrometry, atomic force microscopy, and sheet resistance measurements. Pure Ta–Si films are found to be nanocrystalline. The addition of nitrogen leads to the father process of grain fining resulting in formation of amorphous films with excellent thermal stability. While $Ta_{67}Si_{33}$ starts to crystallize below 700°C, for the most stable $Ta_{34}Si_{25}N_{41}$ layers, crystallisation occurs above 900°C. The films containing more than 40% at. of nitrogen prevent the metallurgical interaction between the metal layer and GaAs and form exceptionally good diffusion barriers above annealing at 800°C.

Методами оберненого резерфордівського розсіяння, рентгенодифракційного аналізу, мас-спектрометрії вторинних іонів, атомно-силової мікроскопії, а також вимірювання поверхневого опору вивчено роль складу в питомому опорі, мікроструктурі та термічній стабільності розпилених Ta–Si–N плівок. Бінарні Ta–Si та потрійні Ta–Si–N тонкі плівки осаджені реактивним високочастотним магнетронним розпиленням мішені Ta_5Si_3 в N_2/Ar газовій суміші. Чисті Ta–Si плівки мали нанокристалічну структуру. Додавання азоту призводить до зменшення розмірів зерен до аморфізації плівок з високою термічною стабільністю. В той час як $Ta_{67}Si_{33}$ починає кристалізуватись нижче від 700°C, кристалізація найбільш стійких

шарів $Ta_{34}Si_{25}N_{41}$ відбувається вище від 900°C. Плівки, що містять більше 40% ат. азоту, запобігають металургійній взаємодії між шаром металу та GaAs, а також утворюють виключно хороші дифузійні бар'єри в результаті відпалу за температури, вищої від 800°C.

Методами обратного резерфордовского рассеяния, рентгенодифракционного анализа, масс-спектрометрии вторичных ионов, атомно-силовой микроскопии, а также измерения поверхностного сопротивления изучена роль состава в удельном сопротивлении, микроструктуре и термической стабильности распыленных Ta–Si–N пленок. Бинарные Ta–Si и тройные Ta–Si–N тонкие пленки осаждены реактивным высокочастотным магнетронным распылением мишени Ta_5Si_3 в N_2/Ar газовой смеси. Чистые Ta–Si пленки имели нанокристаллическую структуру. Добавление азота ведет к уменьшению размера зерен до аморфизации пленок с высокой термической стабильностью. В то время как $Ta_{67}Si_{33}$ начинает кристаллизоваться ниже 700°C, кристаллизация самых устойчивых слоев $Ta_{34}Si_{25}N_{41}$ происходит выше 900°C. Пленки, содержащие больше 40% ат. азота, предотвращают металлургические взаимодействия между слоем металла и GaAs, а также образуют исключительно хорошие диффузионные барьеры при отжиге выше 800°C.

Key words: thin films, magnetron sputtering, microstructure, metallurgical interaction.

(Received April 27, 2004)

1. INTRODUCTION

Initiated by the demands of high temperature and high power III–V electronics, the long-term stability of ohmic and Schottky contact systems on GaAs and different conducting encapsulants, have been extensively studied. These contact layer systems generally include diffusion barrier that prevents the metallurgical reaction between metallization and semiconductor substrate [1]. Various polycrystalline thin films such as TiN [2], HfN [3], and WN [4, 5] have been investigated as diffusion barrier in contact metallization. Among these evaluated films, amorphous thin films are considered as the most promising candidates, because they lack grain boundaries that eliminating fast diffusion paths [6–8].

Recently, amorphous Ta–Si–N films have been one of the most crucial barriers for both Al and Cu metallizations of Si devices [6–11]. They have excellent diffusion barrier properties and thermal/chemical stability against high temperature annealing due to the fact that amorphous to crystalline phase transition takes place above 900°C [6–10, 12].

In a given work, we have investigated the deposition processes and thermal stability of amorphous Ta–Si and Ta–Si–N thin films

on GaAs substrates. This study was focused on the effect of nitrogen content in Ta–Si–N thin films on microstructural, electrical and barrier properties. The failure mechanisms of different Ta–Si–N barriers are also discussed.

2. EXPERIMENTAL

Tantalum-silicon-nitride films were deposited by reactive radio frequency (r.f.) magnetron sputtering method. Sputter deposition was carried out in a gas mixture of N_2 and Ar. For process evaluation and thin film characterization, 100 nm thick films were deposited on semi-insulating GaAs(100)-oriented wafers cleaned using standard procedure [13]. The sputtering conditions used in the work are listed in Table 1.

The film thickness was measurement by Tencor α-step profilometer and film resistivity was calculated from the sheet resistance (R_s) measured by a four-point probe. The electrostatic accelerator Lech at SINS Warsaw was applied to perform the Rutherford backscattering spectrometry (RBS) using the 2 MeV He^+ ions and the $^{14}N(d, \alpha)^{12}$ nuclear reaction analysis (NRA) measurements. Kinetic energy spectra of backscattered ions and the content of nitrogen, as determined by NRA [14], were used with the RUMP code [15] for the elemental analysis.

In order to characterize the thermal stability, Ta–Si and Ta–Si–N films were annealed at 400–1000°C for 5 min in Ar ambient.

Before and after the thermal annealing, the samples were characterized by sheet resistance measurements and secondary-ion mass spectrometry (SIMS) depths' profiling. SIMS analysis was performed with a Cameca 6F instrument with a caesium primary ion beam and detection of CsX^+ secondary cluster ions. The microstructure of thin films was investigated by X-ray diffraction (XRD) using Philips X'Pert–MPD equipment with $CuK_{\alpha 1}$ radiation. The surface morphology of the films was examined using a NanoScope IIIa Dimension 3000TM atomic force microscope (AFM) in taping mode.

TABLE 1. The experimental conditions and deposition parameters.

Target	Ta_5Si_3 (99,95% pure, ∅ 7.5 cm)
Target-to-substrate distance	6.5 (cm)
Initial vacuum	$<1\cdot10^{-6}$ (mbar)
R.F. power	200 (Watts)
Argon flow	100 (sccm)
Nitrogen flow	0–20 (sccm)
Total gas pressure	$4\cdot10^{-3}$ (mbar)

3. RESULTS AND DISCUSSION

3.1. Properties of As-deposited Ta–Si–N Films

The compositions of Ta–Si–N thin films sputter-deposited in various N_2/Ar flow ratios are shown in Fig. 1. The N concentration increase and the atomic ratio Ta/Si decrease with increasing nitrogen-to-argon flow ratio, with a tendency to saturation for large flow ratio. The N content in the films increases from 0 to 50 at.% as N_2/Ar ratio increases from 0 to 20%, because a greater quantity of reactive nitrogen incorporates into the film during the sputtering process. The decrease in the Ta/Si ratio with increasing nitrogen concentration is attributed to differences in sputtering yields of the Ta and Si component with changing sputtering conditions [12].

The inset in Fig. 1 indicates the resistivity of as-deposited Ta–Si–N thin films as a function of N concentration. When the N_2/Ar flow ratio is lower than 10%, the electrical resistivity rose slowly from approximately 270 μΩcm for $Ta_{67}Si_{33}$ film up to 750 μΩcm for the $Ta_{34}Si_{25}N_{41}$ film. However, when the flow ratio is higher than 10%, nitrogen content in the Ta–Si–N films exceeds 40 at.% and the resistivity increases abruptly to 1400 μΩcm and larger. A $Ta_{28}Si_{22}N_{50}$ film has about 38 250

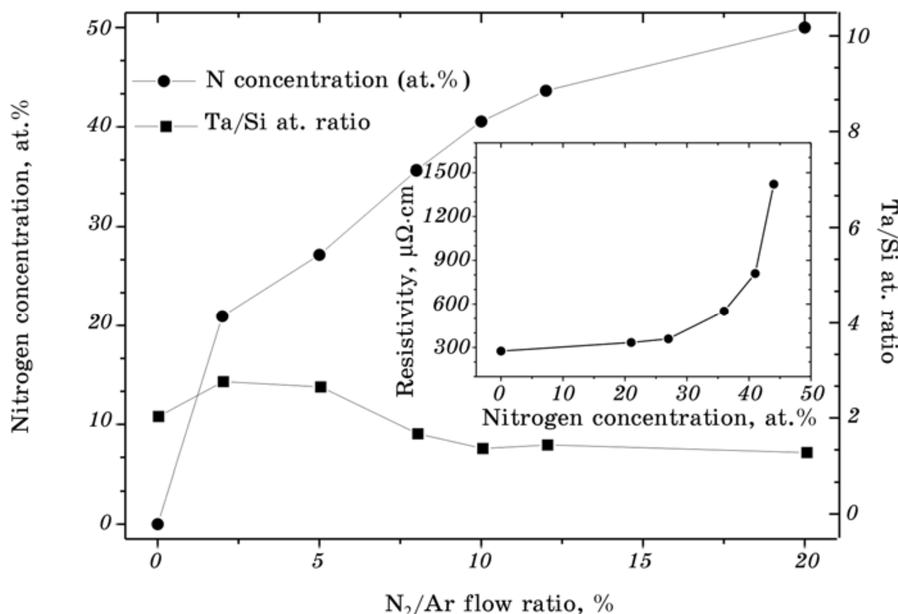

Fig. 1. The nitrogen concentration and Ta/Si atomic ratio as a function of N_2/Ar flow ratio. (Inserted figure: The resistivity as a function of the nitrogen concentration).

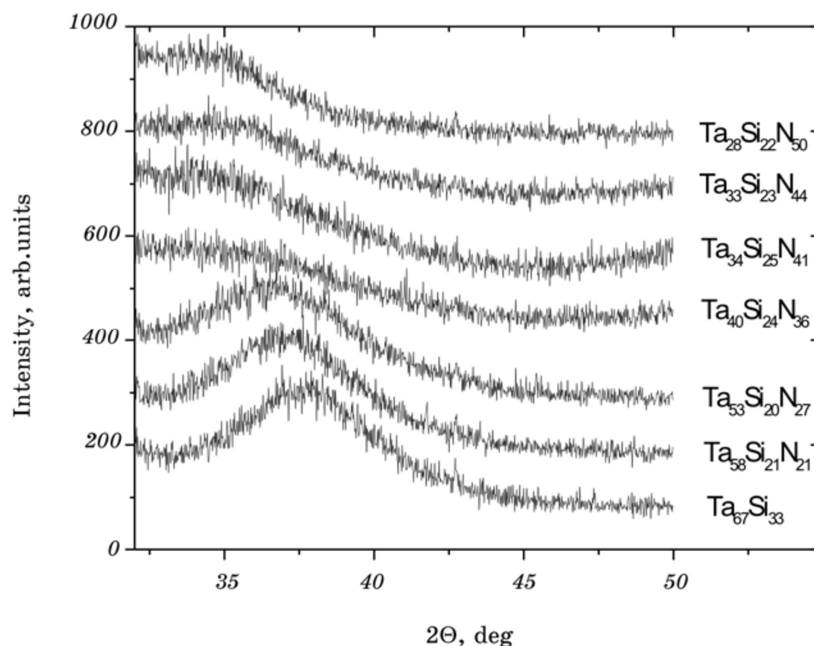

Fig. 2. X-ray diffractograms of Ta–Si–N films sputtered in different N_2/Ar gas mixture.

μΩcm (not shown here). For contacts of submicron dimensions, a films resistivity below about 1000 μΩcm is required [7]. In order to understand the reasons behind the change in film resistivity, the microstructures of these Ta–Si–N films were examined.

Figure 2 shows the X-ray diffraction spectra of the Ta–Si–N films sputtered in various N_2/Ar gas mixtures. The broad peak centred about $2\Theta = 38°$ for the as prepared nitrogen-free film indicate the existence of a nanocrystalline structure as earlier reported in the literature [9, 16]. The addition of N to the Ta–Si films causes a slight shift of the peaks to a lower angle and decreases the intensity, indicated in decreasing grain sizes resulting in amorphous films. Calculations of the mean grain size based on the Scherrer formula give values of approximately 4 and 3 nm, for $Ta_{67}Si_{33}$ and $Ta_{53}Si_{20}N_{27}$ films, respectively. Similar observations have been reported in literature [9, 17, 18]. AFM measurements also suggest that the structure of the Ta–Si–N films is amorphous. As seen in Fig. 3, *a* and Fig. 5, *a*, the sputtered films are nearly free of extended defects and extremely smooth, having a roughness of less than 0.5 nm.

These results suggest that the N impurity suppresses the reaction between Ta and Si and prevents the growth of Ta silicide microcrystallites by the passivation of a grain boundary with N [10]. It has been re-

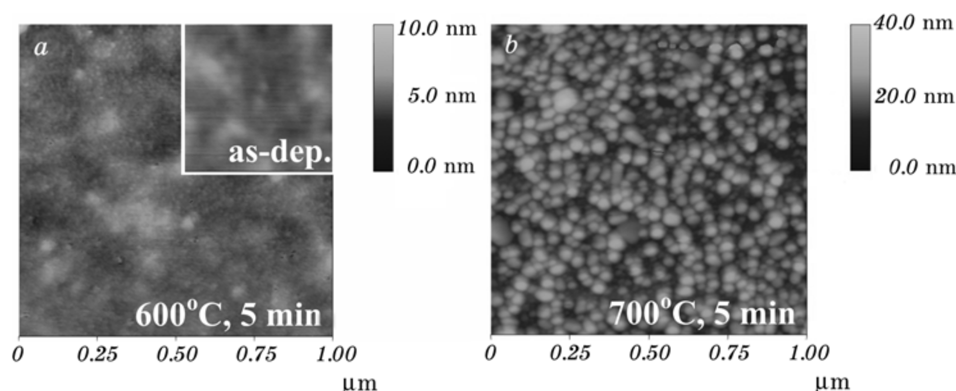

Fig. 3. AFM surface image of GaAs/$Ta_{67}Si_{33}$ samples: *a*—as-deposited and annealed at 600°C for 5 min; *b*—annealed at 700°C for 5 min.

ported that Ta–Si–N films with higher N concentration consisted of a combination Ta–Si, Ta–N and Si–N bonds [12]. The presence of Si–N bonds is attributed to cause the amorphous nature of the high N containing films. The change of structure from nanocrystalline to amorphous correlation with sharply increases in film resistivity.

3.2. Thermal Stability of Ta–Si–N Films

X-ray and resistivity measurements results of GaAs/Ta–Si–N samples annealed at various temperatures are summarized in Table 2.

Investigations concerning the thermal stability of the nitrogen-free layer show the preservation of the nanocrystalline structure up to approximately 600°C. Above this temperature crystallization can be observed resulting in the formation of polycrystalline Ta_5Si_3 and $TaSi_2$.

TABLE 2. Results of X-ray analysis and resistivity measurements of Ta–Si and Ta–Si–N films after annealing at various temperatures.

Thin Film	Microstructure (XRD results)		Resistivity (10^{-3} Ωcm)			
	As-deposited phase	Phases at crystallization temp. (°C)	As-dep.	800°C	900°C	1000°C
$Ta_{67}Si_{33}$	nanocrystalline	Ta_5Si_3, $TaSi_3$ (≈ 700)	0.270	0.170	–	–
$Ta_{34}Si_{25}N_{41}$	amorphous	Ta_5Si_3, $TaN_{0.8}$ (≈ 1000)	0.750	0.750	0.685	0.650

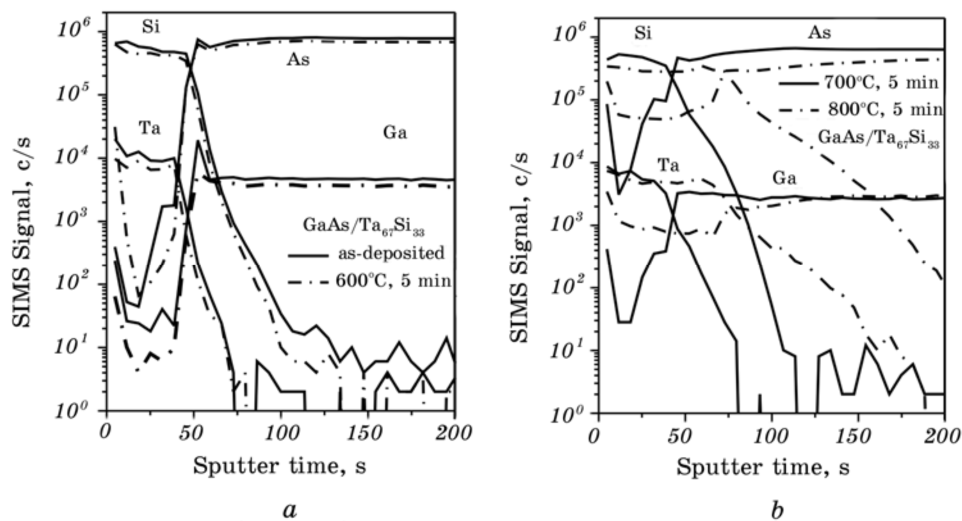

Fig. 4. SIMS profiles of $GaAs/Ta_{67}Si_{33}$ contacts: *a*—as-deposited and annealed at 600°C for 5 min; *b*—annealed at 700 and 800°C for 5 min.

Figure 3 shows surface morphology of $Ta_{67}Si_{33}$ films before and after annealing. The surface of as-deposited films is very smooth with mean roughness about 0.25 nm, and no noticeable change was observed up to 600°C annealing. The roughness increased to 3.5 nm after heat treatment at 700°C and coincided with the growth of 60 nm long crystallites (Fig. 3, *b*).

The influence of heat treatment on composition profiles of $GaAs/Ta_{67}Si_{33}$ contacts is presented in Fig. 4. It shows that the $GaAs/Ta_{67}Si_{33}$ interface remain stable up to annealing at 600°C for 5

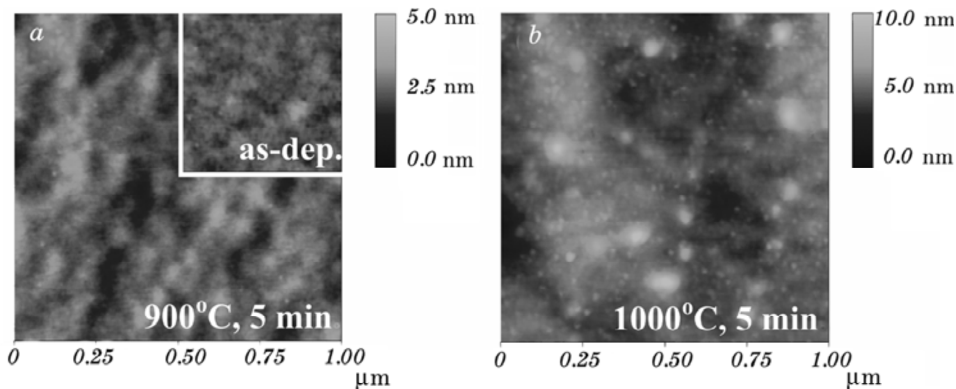

Fig. 5. AFM surface image of $GaAs/Ta_{34}Si_{25}N_{41}$ samples: *a*—as-deposited and annealed at 900°C for 5 min; *b*—annealed at 1000°C for 5 min.

min. At higher-temperature annealing, the SIMS spectra shows significant interdiffusion of the elements at the interface (Fig. 4, *b*).

The X-ray diffraction analysis of $Ta_{34}Si_{25}N_{41}$ films showed no change in phase and structure during the annealing in the range of 500–900°C for 5 min in Ar ambient. The $Ta_{34}Si_{25}N_{41}$ films sputtered at N_2/Ar gas flow ratio of 10% crystallize at about 1000°C and formed polycrystalline Ta_5Si_3 and $TaN_{0.8}$. Figure 5 shows surface morphology of $Ta_{34}Si_{25}N_{41}$ films before and after annealing. The surface of film remained very smooth, with a roughness of about 0.35 nm, even after annealing at 900°C, and did not exhibit features, which could be considered as grain boundaries. However, after heat treatment at 1000°C the roughness increased to 1 nm and crystallites of about 20 nm was observed.

The results of SIMS analyses of GaAs/$Ta_{34}Si_{25}N_{41}$ interface before and after annealing are presented in Fig. 6. It shows that the GaAs/$Ta_{34}Si_{25}N_{41}$ interface remain stable up to annealing temperatures of 800°C. In addition, as shown in Fig. 6, *b*, sharp interface between GaAs and metallization, with no sign of Ga outdiffusion after 900°C annealing is preserved. However, after annealing at 1000°C, SIMS spectra showed significant interface deterioration. The results showed Ta and Si indiffusion, and significant Ga outdiffusion into $Ta_{34}Si_{25}N_{41}$ film.

Thus, $Ta_{67}Si_{33}$ and $Ta_{34}Si_{25}N_{41}$ films, after annealing at temperature above 600 and 900°C, respectively, show crystallized grains. This grain boundary probably was the fast diffusion path, which explains both the outdiffusion of Ga and As and the metallurgical reaction between the metallization and the GaAs substrate.

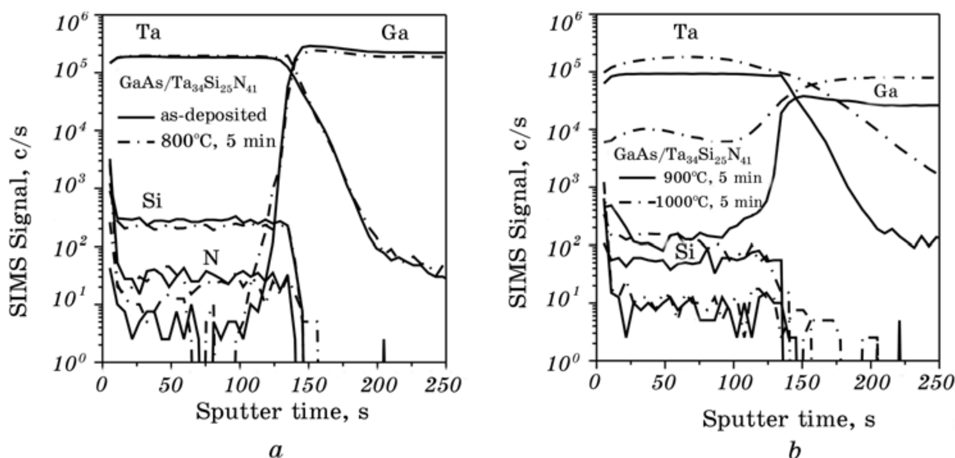

Fig. 6. SIMS profiles of GaAs/$Ta_{34}Si_{25}N_{41}$ contacts: *a*—as-deposited and annealed at 800°C for 5 min; *b*—annealed at 900 and 1000°C for 5 min.

The resistivity of the films before and after annealing is listed in Table 2. The error of the measurement is estimated to be about 10%. The crystallization and/or growth of a finer grain during the annealing is believed to be responsible for the decrease in the film resistivity from 270 μΩcm to 170 μΩcm for the $Ta_{67}Si_{33}$ film annealed at 800°C, and from 750 μΩcm to 650 μΩcm for the $Ta_{34}Si_{25}N_{41}$ film annealed at 1000°C. The drop in film resistivity of $Ta_{34}Si_{25}N_{41}$ after annealing at 900°C may be explained by a relaxation of the atomic disorder in amorphous materials.

4. CONCLUSION

Tantalum-silicon-nitrogen thin film with excellent diffusion barrier properties was reactive r.f. sputter deposited onto GaAs(100) substrate using a Ta_5Si_3 target in a mixture of Ar (100 sccm) and N_2 (10 sccm) gases at a total pressure of $4\cdot10^{-3}$ mbar. The as-deposited $Ta_{34}Si_{25}N_{41}$ film was amorphous and crystallizes at 1000°C, as identified by X-ray diffraction analysis. The resistivity of $Ta_{34}Si_{25}N_{41}$ film of about 750 μΩcm is adequate for contacts of submicron dimensions. XRD, AFM, and SIMS results indicate that $Ta_{34}Si_{25}N_{41}$ is thermally stable on GaAs up to 800°C. Results of [19] show that 100 nm thick $Ta_{34}Si_{25}N_{41}$ diffusion barriers prevent interdiffusion between Au and GaAs up to 800°C and can be used in the application of high temperature electronics.

ACKNOWLEDGEMENTS

The work was supported by the grant from the NATO (NUKR.RIG 981275), and one author (A. V. Kuchuk) was supported by the research grant of N.A.S.U. for young scientists.

REFERENCES

1. M.-A. Nicolet, *Thin Solid Films*, **52**: 415 (1978).
2. K. Yokota, K. Nakamura, M. Satho et al., *Thin Solid Films*, **406**: 87 (2002).
3. R. Nowak and C. L. Li, *Thin Solid Films*, **305**: 297 (1997).
4. F. C. T. So, E. Kolawa, X. A. Zhao et al., *Thin Solid Films*, **153**: 507 (1987).
5. E. Kolawa, F. C. T. So, J. L. Tandon et al., *J. Electrochem. Soc.*, **134**: 1759 (1987).
6. E. Kolawa, J. M. Molarius, C. W. Nieh et al., *J. Vac. Sci. Technol. A*, **8**, No. 3: 3006 (1990).
7. M.-A. Nicolet, *Appl. Surf. Sci.*, **91**: 269 (1995).
8. M.-A. Nicolet, *Defect and Diffusion Forum*, **143–147**: 1271 (1997).
9. D. Fischer, T. Scherg, J. G. Bauer et al., *Microelectron. Eng.*, **50**: 459 (2000).

10. D. J. Kim, Y. T. Kim, and Y. W. Park, *J. Appl. Phys.*, **82**, No. 10: 4847 (1997).
11. Y. J. Lee, B. S. Suh, M. S. Kwon et al., *J. Appl. Phys.*, **85**, No. 3: 1927 (1999).
12. Y. S. Suh, G. Heuss, and V. Misra, *J. Vac. Sci. Technol. B*, **22**, No. 1: 175 (2004).
13. E. Kaminska, A. Piotrowska, and E. Mizera, *Thin Solid Films*, **246**: 143 (1994).
14. G. Amsel and D. David, *Rev. Phys. Appl.*, **4**: 383 (1969).
15. L. R. Doolittle, *Nucl. Instrum. Methods B*, **9**: 334 (1985).
16. Y. J. Lee, B. S. Suh, and C. O. Park, *Thin Solid Films*, **357**: 237 (1999).
17. E. Ivanov, *Thin Solid Films*, **332**: 325 (1998).
18. C. Linder, A. Dommann, and G. Staufert, *Sens. Actuators. A*, **61**: 387 (1997).
19. A. Kuchuk, E. Kaminska, A. Piotrowska et al., *Thin Solid Films*, (2004) (in press).